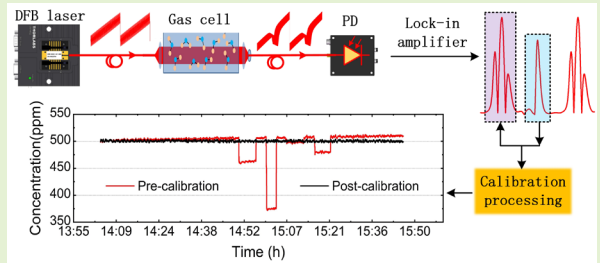


Self-calibrated Method for WMS Gas Sensor Immune to Optical and Electronic Drift

Fupeng Wang, Jinghua Wu, Qiang Wang, Qian Li, Diansheng Cao, and Qingsheng Xue

Abstract—A novel self-calibrated method is proposed for wavelength modulation spectroscopy (WMS) system to improve the long-term stability for gas detection. In the method, the absorption-induced 2nd harmonic is normalized by an absorption-independent pulse signal. Since the 2nd harmonic and pulse signal are demodulated by the same lock-in amplifier, they are completely homologous regardless of the optical path or the circuitry. As a result, the influence on gas detection coming from the optical and electronic drift can be effectively suppressed. In the experiment, a WMS-based CH₄ detection system using a 1653nm laser is constructed to verify the reliability of the new method. For detection of 500 ppm CH₄ sample, more than 100 ppm measurement error coming from artificial fiber loss can be eliminated with this method. In continuous detection of 2 hours, 8.97 ppm (1.79%) measurement drift is observed from 501.07 ppm to 510.04 ppm. However, the drift is reduced to 0.95 ppm (0.19%) after applying the self-calibrated method. Comparative experiment with the 2f/1f technique indicates that the proposed self-calibrated method has a commensurate ability for interference cancellation.



Index Terms—Wavelength modulation spectroscopy (WMS), self-calibration, gas sensor, optical fluctuation, electronic drift.

I. Introduction

SPECTROSCOPY has emerged as a highly sensitive and selective technique to provide real-time analysis with miniaturization potential and low power consumption for applications in air quality detection, medical diagnosis, and industrial emission detection [1]-[6]. Over the last decades, tunable diode laser absorption spectroscopy (TDLAS) stands out as a robust technique to measure gas characteristics in real-time. Light emitted from tunable diode sources passes through a gas sample to a photodetector, and the absorption of light can be related to the gas temperature, pressure and species concentration using spectral absorption models of the target species. Generally, the TDLAS mainly includes direct absorption spectroscopy (DAS) [7][8] and wavelength modulation spectroscopy (WMS) [9]-[11]. In DAS-based systems, laser wavelength is tuned with a scanning ramp to overlap the absorption line of target gas sample and absorption-

induced intensity concavity would appear on the photo-detected signal. Then, differential strategies based on hardware circuits or software algorithm are performed to demodulate the absorption profile and non-absorption baseline [12]. The DAS-based system is very simple and cost-effective, but it is noise-sensitive so that it has limitations for high sensitivity trace gas detection. To deal with the noise issue of DAS-based system, averaging algorithm is a frequently used method which is easy and effective. However, in some systems where the wavelength scanning frequency of light source is limited, massive averaging process would decrease the response speed of measurement system. Afterwards, the WMS is proposed as a better method for trace gas detection since it enables the detection of weak absorption with a high signal to noise ratio (SNR). In a WMS-based system, a high-frequency modulation signal is introduced in addition to the scanning ramp to bring the detection to a higher frequency range. Absorption-induced

This work was supported in part by the National Natural Science Foundation of China under Grant 52001295, 62005267 and 62375262; in part by the Natural Science Foundation of Shandong Province under Grant ZR2020QF097 and Grant ZR2021QD140; in part by the Open Fund of State Key Laboratory of Applied Optics under Grant SKLAO2021001A12; in part by the Central University Basic Research Fund of China under Grant 202013024 and Grant 202065004; and in part by Key Research and Development Program of Shandong Province, under Grant 2020CXGC010706. (Corresponding author: Fupeng Wang, Qingsheng Xue)

Fupeng Wang is with the Faculty of Information Science and Engineering, Engineering Research Center of Advanced Marine

Physical Instruments and Equipment, Ocean University of China, Qingdao 266100, China, and also with the State Key Laboratory of Applied Optics, Changchun Institute of Optics, Fine Mechanics and Physics, Chinese Academy of Sciences, Changchun 130033, China (e-mail: wfp@ouc.edu.cn).

Qiang Wang is with the State Key Laboratory of Applied Optics, Changchun Institute of Optics, Fine Mechanics and Physics, Chinese Academy of Sciences, Changchun 130033, China.

Jinghua Wu, Qian Li, Diansheng Cao and Qingsheng Xue are with the Faculty of Information Science and Engineering, Engineering Research Center of Advanced Marine Physical Instruments and Equipment, Ocean University of China, Qingdao 266100, China.

harmonic signals are measured by a lock-in amplifier to indicate the gas characteristics. Thus, the low-frequency noise (e.g., 1/f noise) is eliminated and white noise (e.g., thermal noise and shot noise) is substantially reduced as well. As a result, the gas detection limit and sensitivity are all improved to a better level. Even though, high-precision quantitative measurement is still full of challenges in harsh environments, whether DAS or WMS is used. Generally, standard gas sample with a known concentration and pressure is carried to periodically calibrate the system [13], which increases the system complexity and measuring uncertainty. However, in specific harsh environment, the standard gas sample is unavailable, meanwhile the optical intensity and electronic measurement are very unstable. For example, the scenario involved in combustion analysis [14]-[16] is such a harsh environment, including the applications of coal-fired furnace monitoring [17], detonation engine analysis [18], exhaust plume measurement [19], etc. In such above conditions, the characteristics of light transmission medium (combustion field) undergo drastic changes, resulting in that the photo-detected signals contain lots of fluctuations. In addition, the mechanical vibration of such experiment platform is also very violent. Another example is the outdoor long-distance fiber optic distributed measurement network, the optical intensity fluctuation and circuit drift are very frequent due to the climate change and human activities. To deal with the above problems, frequent calibration is time-consuming and ineffective sometimes.

To address the challenges associated with the optical intensity fluctuation, researchers have developed a variety of automatic calibration methods and calibration-free techniques in recent years. The most common approach is to simultaneously measure the non-absorption optical intensity to monitor the optical fluctuation and use the monitored signal to calibrate the detected results [8][20]. Tu et al. [21] utilized the linear relationship between multiple frequency peaks in the power spectral density of demodulated second harmonic signals to address light intensity fluctuations. By analyzing the relationship between these signals and the incident light intensity, real-time correction of optical intensity fluctuations was achieved, resulting in a high SNR across a wide range of light intensities. As to the calibration-free techniques, researchers from Hanson's group of Stanford university proposed a calibration-free WMS technique, known as CF-WMS, which normalizes the WMS-2f signal to the first harmonic (1f) for gas concentration measurement in harsh environments [22]. The CF-WMS eliminates the need for field calibration, resulting in improved accuracy and stability. Additionally, normalizing the WMS-2f signal over the 1f signal reduces the sensitivity to laser intensity fluctuation, further enhancing the measurement accuracy and stability. Afterwards, the 2f/1f strategy is widely applied to WMS-based systems to improve its robustness, especially for the field of combustion diagnosis [23][24]. Kyle Owen [25] developed a calibration-free ammonia sensor using WMS-2f/1f technique, enabling real-time detection of ammonia concentration in exhaled gas without the inconvenience and errors associated with periodic calibration. Recently, Liu et al. [26] introduced a self-calibrated WMS method, in which two approaches were used to observe the simulated calibration curves, described as the WMS-2f/1f amplitude and WMS-2f/1f integral area. Compared with the

2f/1f amplitude implementation, the 2f/1f integral area improves the detection precision and long-term stability. Besides, the measurement error caused by wavelength drift is reduced as well. As reviewed above, the automatic calibration methods and calibration-free techniques have been verified that are effective to eliminate influence from optical fluctuation. Especially the 2f/1f strategy from Hanson group has been verified robust as a "gold standard" by many studies and widely applied to engineering. In addition to the optical fluctuation, circuit drift is another tricky problem which limits the performance of gas sensing system. In many published papers, while the minimum detection limit (MDL) for gas detection has been improved to part-per-billion (ppb) and part-per-trillion (ppt) level [27][28]. Without temperature and pressure control, few WMS systems were reported to achieve ppb or ppt level in terms of repeatability and long-term stability to our knowledge. Engineers are all familiar with that the long-term indicators (e.g., repeatability and stability) are much more challenging to achieve compared to transient indicators (e.g., sensitivity and MDL). The reason is that electronic parameters would drift due to temperature variations and device aging. Therefore, other than optical intensity fluctuation, electronic drift deserves our attention as well in order to further enhance the long-term stability of WMS gas sensing systems. Even commercial temperature controller is easy to obtain nowadays. However, temperature controlling system is often highly power consuming which limits its application of intrinsic safety. So, calibration techniques are still needed and worth studying.

In this study, we propose a new self-calibrated method for WMS-based gas detection systems, which enables the measurement immune to both the optical and electronic drift. The rest of this study is organized as follows. Section 2 introduces the fundamentals of the self-calibrated method. Section 3 demonstrates the experiment system and how the experiment conducted. Section 4 presents the experimental results and gives an analysis. In the end, section 5 concludes this study.

II. FUNDAMENTAL OF THE SELF-CALIBRATED WMS METHOD

The self-calibrated method is proposed for WMS-based gas detection systems. Therefore, the WMS principle is introduced to aid the fundamental demonstration. In this method, a low-frequency sawtooth wave superimposed with a high-frequency sinusoidal signal is used to drive the laser source, enabling the wavelength scanning and modulation of laser output. The output optical frequency $\nu(t)$ and intensity $I_0(t)$ can be presented as follows.

$$\begin{aligned} \nu(t) &= \bar{\nu}(t) + \delta\nu \cdot \cos(\omega t) \quad (1) \\ I_0(t) &= \bar{I}(t) + \Delta I_1 \cdot \cos(\omega t + \varphi_1) + \Delta I_2 \cdot \cos(2\omega t + \varphi_2) \quad (2) \end{aligned}$$

Where $\bar{\nu}(t)$ is the center frequency of wavelength modulation which changes slowly over time according to the scanning pattern of sawtooth wave, $\delta\nu$ represents the wavelength modulation amplitude, ω is the modulation frequency meeting the equation of $\omega=2\pi f$ where f is the modulation frequency in unit of Hz. $\bar{I}(t)$ is the optical intensity which changes slowly according to the scanning pattern of

sawtooth wave as well, ΔI_1 and ΔI_2 are modulation amplitudes of optical intensity from first-order linear and second-order nonlinear response. φ_1 and φ_2 are phase shifts between wavelength and intensity response. To simplify the following demonstration, the minor second-order nonlinearity is eliminated, then the photo-detected signal $I_s(t)$ after gas absorption can be expressed based on the Beer-Lambert law:

$$I_s(t) = [\bar{I}(t) + \Delta I_1 \cdot \cos(\omega t + \varphi_1)] \cdot \exp[-PS(T)XL\Phi(v)] \quad (3)$$

Where P is the pressure, $S(T)$ is the line strength of molecular absorption spectrum which is related to thermodynamic temperature T , X denotes the molecular fraction of test gas, L represents the absorption path length, $\Phi(v)$ is the line function of absorption profile. As shown in Fig. 1, there is a sharp falling edge between adjacent cycles of the sawtooth wave. In order to reflect this sharp change in photo-detected signal, we use an impulse function to represent it and rewrite Eq. (3) as:

$$S_2 = \underbrace{G \cdot [\bar{I}(t) \cdot H_2 \cdot \cos(\Delta\phi_1) + \Delta I_1 \cdot H_1 \cdot \cos(\Delta\phi_2) + \Delta I_1 \cdot H_3 \cdot \cos(\Delta\phi_3)]}_{H_{2nd}} + \underbrace{G \cdot I_p \cdot [h_1 \cdot \cos(\Delta\psi_1) + h_3 \cdot \cos(\Delta\psi_3)]}_{H_p} \quad (6)$$

where G is the electronic coefficient which includes the gain of photodetection circuit and lock-in amplifier, so any electronic fluctuation would be reflected by this factor G . The phases of $\Delta\phi_1, \Delta\phi_2, \Delta\phi_3, \Delta\psi_1, \Delta\psi_3$ are phase difference between the target harmonic components and the reference signal of lock-in amplifier. Obviously, the first item H_{2nd} coming from the gas absorption is useful for concentration inversion, however, the second item H_p is absorption-independent which comes from the signal mutation between adjacent sawtooth cycles as shown

$$I_s(t) = [\bar{I}(t) + \Delta I_1 \cdot \cos(\omega t + \varphi_1)] \cdot \exp[-PS(T)XL\Phi(v)] + I_p \cdot \delta(t) \cdot \cos(\omega t + \varphi_1) \quad (4)$$

where I_p is the peak-to-peak value of sawtooth wave as depicted in Fig. 1, which represents the amplitude of the impulse function, $\delta(t)$ is the impulse function. To expand the absorption item in scanning range and impulse function item at falling edge using Fourier series, the Eq. (4) can be further expressed as:

$$I_s(t) = [\bar{I}(t) + \Delta I_1 \cdot \cos(\omega t + \varphi_1)] \cdot \sum_{k=0}^{\infty} H_k \cos(k\omega t) + I_p \cdot \sum_{k=0}^{\infty} h_k \cos(k\omega t) \cdot \cos(\omega t + \varphi_1) \quad (5)$$

where H_k and h_k are the k -order Fourier components of absorption profile and impulse function respectively [29]. In WMS-based gas detection systems, a lock-in amplifier is commonly used to demodulate the second harmonic signal S_2 of photo-detected signal $I_s(t)$ for concentration inversion, and the second harmonic results can be expressed as:

in Fig. 1.

In the previous studies, we all agree with that the pulse signal H_p is useless, and even harmful for absorption-dependent second harmonic detection, especially for low concentration detection, the pulse signal may distort the useful second harmonic signal. However, we utilize the pulse signal to calibrate the second harmonic signal to eliminate the impact of drift from optical intensity and electronic circuit in this study. To make it clearer, the Eq. (6) can be further normalized by optical intensity as:

$$S_2 = \underbrace{G \cdot I_{laser} [s(t) \cdot H_2 \cdot \cos(\Delta\phi_1) + p_1 \cdot H_1 \cdot \cos(\Delta\phi_2) + p_1 \cdot H_3 \cdot \cos(\Delta\phi_3)]}_{H_{2nd}} + \underbrace{G \cdot I_{laser} \cdot p_2 [h_1 \cdot \cos(\Delta\psi_1) + h_3 \cdot \cos(\Delta\psi_3)]}_{H_p} \quad (7)$$

$$\begin{cases} p_1 = \frac{\Delta I_1}{I_{laser}} \\ p_2 = \frac{I_p}{I_{laser}} \\ s(t) = \frac{\bar{I}(t)}{I_{laser}} \end{cases} \quad (8)$$

where p_1 and p_2 are proportionality coefficient, I_{laser} denotes the maximum optical intensity received by the photodetector, $s(t)$ is the normalized sawtooth signal. Thus, any fluctuations in optical path would be reflected in I_{laser} and any drift in electronic circuit would be reflected in gain coefficient G .

$$S_{out} = \frac{H_{2nd}}{H_p} = \frac{G \cdot I_{laser} [s(t) \cdot H_2 \cdot \cos(\Delta\phi_1) + p_1 \cdot H_1 \cdot \cos(\Delta\phi_2) + p_1 \cdot H_3 \cdot \cos(\Delta\phi_3)]}{G \cdot I_{laser} \cdot p_2 [h_1 \cdot \cos(\Delta\psi_1) + h_3 \cdot \cos(\Delta\psi_3)]} = \frac{[s(t) \cdot H_2 \cdot \cos(\Delta\phi_1) + p_1 \cdot H_1 \cdot \cos(\Delta\phi_2) + p_1 \cdot H_3 \cdot \cos(\Delta\phi_3)]}{p_2 [h_1 \cdot \cos(\Delta\psi_1) + h_3 \cdot \cos(\Delta\psi_3)]} \quad (9)$$

As shown in Eq. (9), the interference variate from optical path and circuit can be eliminated by deleting G and I_{laser} , the absorption information is only included in the item of H_1, H_2, H_3 and the rest items are all constant. Compared with 2f/1f calibration-free technique, this method is expected to achieve both elimination of circuit drift and optical fluctuations, since the absorption-dependent 2nd harmonic signal H_{2nd} and pulse signal H_p are demodulated by the same lock-in amplifier channel, they are completely homologous regardless of the

Absorption-dependent information is involved in item H_{2nd} for gas concentration detection, and item H_p has nothing to do with the gas absorption. So, we plan to use item H_p to calibrate the signal H_{2nd} as:

optical path or the circuitry. Furthermore, the self-calibrated method only needs a single lock-in amplifier channel. As displayed in Fig. 1, sawtooth-scanned WMS strategy is simulated based on MATLAB software, the absorption induced second harmonic signal H_{2nd} and the pulse signal H_p are observed in the simulation. Furthermore, the second harmonic amplitude decreases when we artificially attenuate the photo-detected signal from I_{p1} to I_{p2} , simultaneously, amplitude of the pulse signal also decreases in sync. This gives our confidence that the calibration method demonstrated above

would be effective for WMS-based detection. Of course, it still has limitation in the method that the measured pulse signal H_p must be absorption-independent to guarantee the reliability of calibration. Considering that the molecular absorption line has a broadening effect, so the pulse signal H_p inevitably has a little of absorption information. As a result, it would affect the effectiveness of calibration. To ensure that the pulse signal H_p is independent of absorption to the maximum extent possible, a wide wavelength scanning should be realized by the sawtooth ramp in this method. This is a necessary condition.

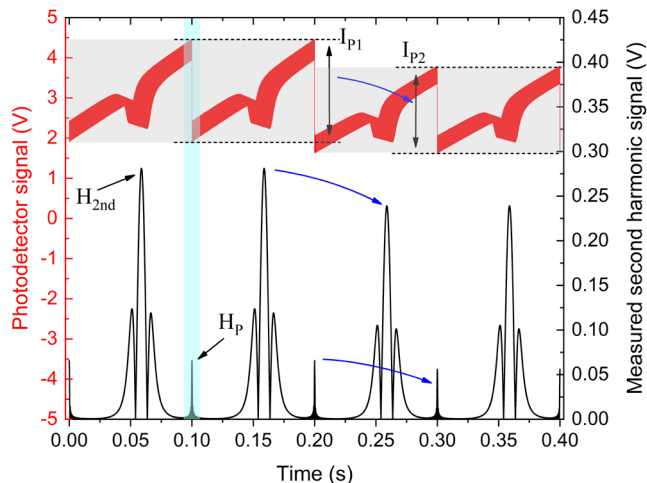


Fig. 1. Simulated photo-detected signal and demodulated second harmonic signal from a WMS-based system.

III. EXPERIMENT SETUP

To verify the self-calibrated method as demonstrated in section 2, a sawtooth-scanned WMS-based CH₄ detection is constructed as depicted in Fig. 2, a continuous wave (CW) fiber coupled distributed feedback (DFB) laser with a wavelength of 1653 nm is used as the probe light source. A commercial laser controller (Stanford Research Systems, LDC501, USA) is used to control the driving current and laser temperature. A commercial DAQ card (National Instruments, USB-6361, USA) is employed to realize the signal generation and digital lock-in amplifier. Sawtooth wave in 10 Hz superimposed with 4 kHz sinusoidal signal (Fig. 2a) is generated to drive the DFB laser. The output laser beam is connected to a fiber-coupled multi-pass gas cell (3 m optical path) for gas detection, in which photon energy is absorbed by the target molecules. The transmitted light signal is converted into voltage by a InGaAs photodetector and a home-made transimpedance amplifier (TIA), the TIA uses a 10 kΩ resistance to realize I-V conversion. The output signal of TIA is displayed in Fig. 2b, which is collected with a sampling rate of 2 MS/s by USB-6361 for lock-in detection, 4-order Bessel low-pass filter is programmed in the digital lock-in amplifier and its 3dB bandwidth is 50 Hz. A demo of the demodulated second harmonic curve is plot in Fig. 2c. A fiber attenuator is inserted to the optical path to artificially introduce optical fluctuation, a varistor is installed at the second stage of the TIA to provide 1-50 gain factor, and simulate the circuit drift by adjusting the gain. Thus, both optical and electronic drift can be artificially controlled to verify the effectiveness of the self-calibrated method.

Methane gas is chosen in this study to verify the new method. Considering that most of the TDLAS-based CH₄ sensors are developed by utilizing the overtone band of CH₄ due to the matured semiconductor laser and detector technologies in near infrared (NIR) region, a 1653 nm DFB laser is chosen as the light source. The absorption coefficient of 1 ppm CH₄ is simulated in the range of 6030-6070 cm⁻¹ according to the HITRAN database. To check the potential interference from background gases, 4000 ppm H₂O and 500 ppm CO₂ are also simulated in the same NIR region as shown in Fig. 3. Obviously, 1653.72 nm (6046.96 cm⁻¹) and 1650.96 nm (6057.08 cm⁻¹) are two ideal choices for CH₄ detection. However, the 1650.96 nm is out of the operating range of our DFB laser. So, parameters are modulated by USB-6361 and LDC501 to make the DFB laser to select the CH₄ absorption line at 1653.72 nm in the experiment.

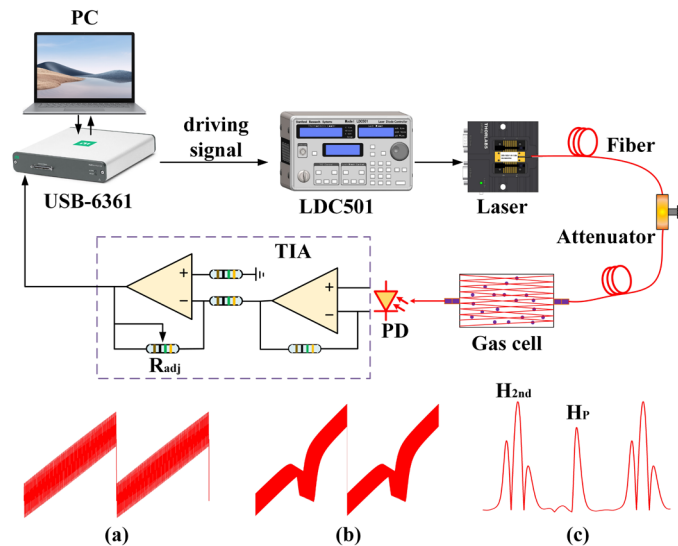


Fig. 2 Schematic of the experimental system. (a) Laser driving signal, (b) Photo-detected absorption signal after TIA circuit, (c) Demodulated second harmonic signal which includes the absorption-dependent component H_{2nd} and absorption-independent pulse signal H_p .

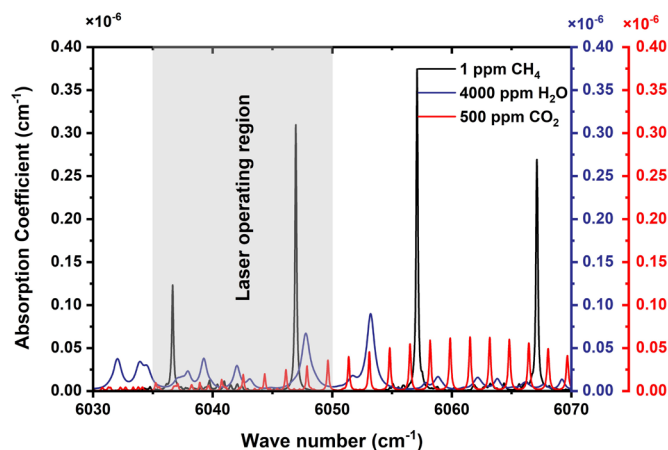


Fig. 3 Simulated absorption coefficient of 1 ppm CH₄, 4000 ppm H₂O and 500 ppm CO₂ at 1 bar and 296 K. Shadow zone: wavelength output range of the DFB laser in our lab is 1652-1657 nm.

IV. EXPERIMENT RESULTS ANALYSIS

In the start of experiment, we expect to observe the

phenomenon as simulated in Fig. 1 for the first step verification. A sample CH₄ of 500 ppm concentration is provided and infused to gas cell for measurement. The demodulated second harmonic data is stored on a personal computer (PC) by LABVIEW software and plotted in Fig. 4. As demonstrated in section 2, the absorption-dependent second harmonic signal H_{2nd} and absorption-independent pulse signal H_p are really observed as depicted on the left of Fig. 4. Afterwards, we manually increase the fiber loss by adjusting the fiber attenuator and increase the TIA gain by adjusting the varistor, the second harmonic signal H_{2nd} decreases and increases respectively. Simultaneously, amplitude of pulse signal decreases and increases too as labeled in Fig. 4. In other words, this preliminary evidence demonstrates that the amplitude of the pulse signal synchronously varies with optical fluctuation and circuit drift, giving our confidence that the pulse signal can be used as a reference to do the calibration.

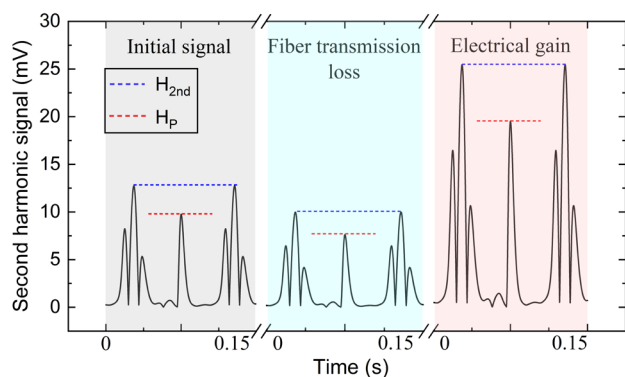


Fig. 4 The detected second harmonic curve, including the absorption-dependent H_{2nd} and absorption-independent H_p , when changing the fiber transmission loss and electrical gain.

To display the calibration process, we continuously vary the fiber loss and circuit gain artificially, during which the original photo-detected signals and second harmonic signals are saved and plotted as shown in Fig. 5a. It is indicated that the photo-detected signal changes when the artificial interference is introduced, as a result, the second harmonic amplitude changes as well. Obviously, the change in second harmonic amplitude does not originate from concentration variations, but rather from variations in the received optical intensity of photodetector or drift in the circuit gain. Thus, the optical and electronic drift would lead to misleading results in the concentration inversion. Fortunately, the results in Fig. 5a also reveal that the changing tendency of the pulse amplitude is consistent with the second harmonic amplitude. So, the pulse amplitudes are used to calibrate the second harmonic signals and the calibrated results are plotted in Fig. 5b. In accordance with expectation, the post-calibration second harmonic signals align well which means the pulse-signal-based calibration method works effectively.

To evaluate the improvement of proposed self-calibrated method for CH₄ detection in ppm unit, a series of CH₄ concentrations is provided to do the linear test by controlling the mixture ratio of pure nitrogen and 1% CH₄, including 9 concentrations of 5 ppm, 10 ppm, 20 ppm, 50 ppm, 100 ppm, 500 ppm, 1000 ppm, 1500 ppm and 2000ppm. As a result, a sensitivity of 26 μ V/ppm is achieved with a linear fitting R-

Square of 0.99952.

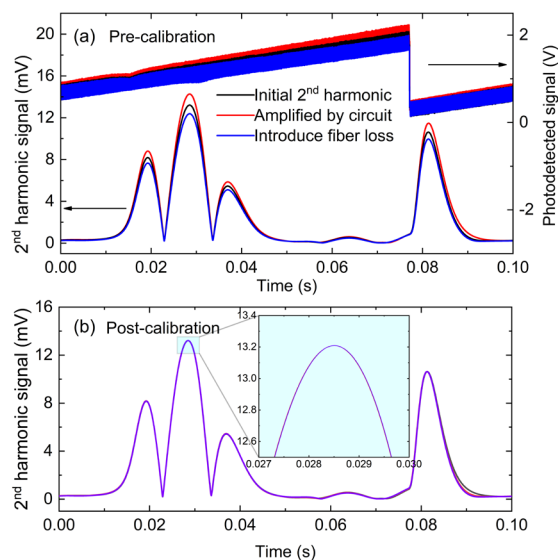


Fig. 5 The calibration process based on 500 ppm CH₄ sample. (a) The original photo-detected signal and corresponding second harmonic signals when artificial disturbance is introduced. (b) The calibrated results of second harmonic signals.

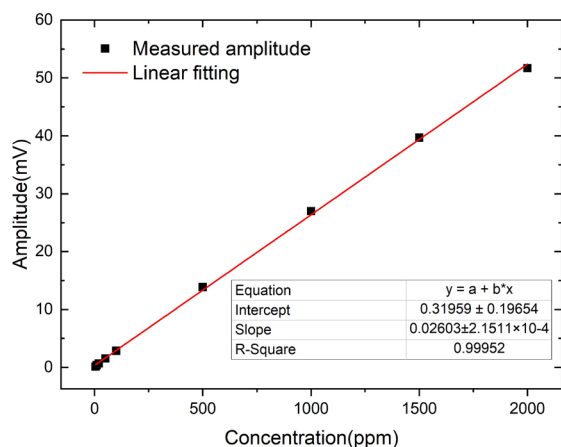


Fig. 6 The linear test of nine CH₄ concentrations of 5 ppm, 10 ppm, 20 ppm, 50 ppm, 100 ppm, 500 ppm, 1000 ppm, 1500 ppm and 2000ppm.

Considering the practical application scenarios, most optical fluctuation and circuit drift are introduced gradually which come from the transmission loss and temperature drift, because the output power of DFB laser itself is highly stable. Of course, in some long-distance distributed fiber sensing systems, external factors induced fiber stress or fiber bending may significantly alter the efficiency of light transmission, resulting in big changes in photo-detected signals. To simulate the violent fluctuation occurred in harsh environment, we artificially introduce disturbance to optical path and electric circuit by bending the fiber and adjusting the gain factor during a 2-hour measurement. Additionally, drift in measured signal caused by gradual changes in the optical path and circuit is also observed as shown in Fig. 7. Throughout the entire experimental process, the CH₄ concentration remains constant at 500 ppm. The second harmonic amplitude and pulse signal amplitude are synchronously collected for nearly 2 hours and plotted in Fig. 7a, at the time points marked with black arrows,

we intentionally introduce significant optical fluctuations. It is evident that the amplitude of pulse signal H_p and the amplitude of the absorption-induced second harmonic signal H_{2nd} are perfectly synchronized. In the next step, the pulse signal amplitude is used to normalize the second harmonic signal and the result is displayed in Fig. 7b, the absorption-unrelated interferences have been effectively suppressed, whether they are intentionally introduced or originated from system drift. The original signal without calibration is also plotted in the same figure as a comparison, during the 2-hour period the measured concentration changes from 501.07 ppm to 510.04 ppm, a 1.79% drift is observed in the 2 hours. However, such measurement drift is improved to 0.19% (from 500.85 ppm to 499.9 ppm) by the self-calibrated method. In addition, artificial optical fluctuations cause measurement errors of more than 100 ppm in the experiment, however, such significant errors can be completely suppressed by the new method. Standard deviation 1σ before and after calibration is also calculated and compared, which indicates that the self-calibrated method has no negative impact on the measurement sensitivity.

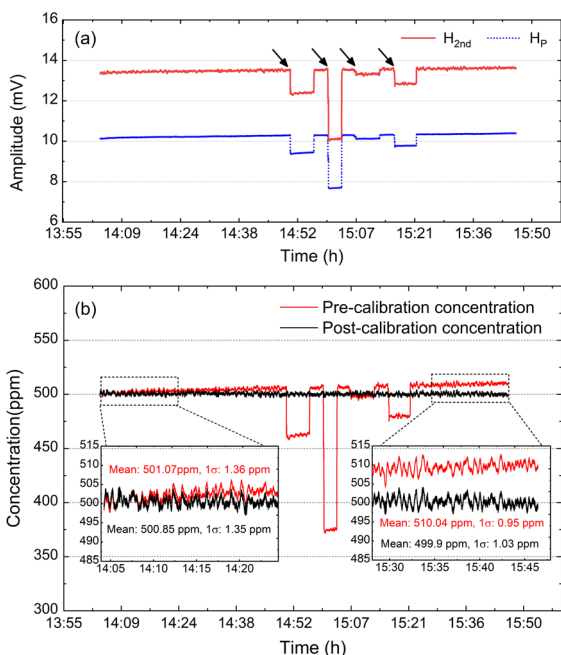


Fig. 7 Comparison of CH₄ detection stability based on a 2-hour long-term experiment between with and without self-calibrated method. (a) Long-term recorded second harmonic amplitude and pulse signal amplitude, (b) The concentration measurement drift analysis.

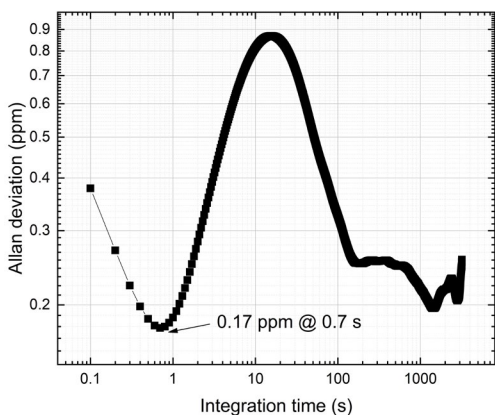


Fig. 8 Allan deviation analysis

To further evaluate the stability of the proposed self-calibrated method, Allan deviation analysis is performed based on the 2 hours post-calibration data in Fig. 7b, the results are plotted in Fig. 8. A minimum detection limit of 0.17 ppm is achieved at an integration time of 0.7 s. In addition, all the Allan deviation values are below 0.9 ppm during the period of > 1 hour, which means the calibrated results by the self-calibrated method have a good long-term stability.

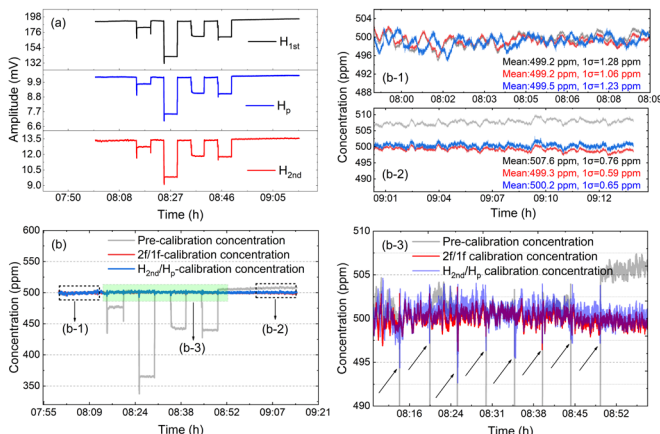


Fig. 9 Comparative experiment between the proposed self-calibrated method and 2f/1f technique. (a) Measured absorption-induced first harmonic signal H_{1st} and second harmonic signal H_{2nd} , and the absorption-independent pulse signal H_p . (b) Comparison results between self-calibrated method and 2f/1f technique. (b-1, b-2, b-3) The drawing of partial enlargement of figure 9 (b).

As shown in Fig. 7, the self-calibrated method has been preliminarily verified to be effective compared with free-running WMS system without any calibration processing. Highly stable results are measured in a long-term experiment, which is immune to the optical and electronic drift. To make the verification study more convincing, a comparison experiment is supplemented to compare the performance between the self-calibrated method and the widely applied 2f/1f technique. In the experiment, a CH₄ sample gas in concentration of 500 ppm is still used and kept constant throughout the entire measurement. Similarly, we bend the fiber and adjust the TIA gain factor to artificially introduce disturbance to simulate the harsh environment. To realize the 2f/1f technique, another channel of digital lock-in amplifier is programed based on the DAQ card. Thus, absorption-induced 1st and 2nd harmonic signals and absorption-independent pulse signal are recorded in the same time as shown in Fig. 9a. Similar to the Fig. 7a, the measured results in Fig. 9a also show good consistency among H_{1st} , H_p and H_{2nd} when interference is introduced to the sensing system, which means both H_{1st} and H_p signals can be used as a reference to calibrate the absorption-induced H_{2nd} . Calibration results based on the self-calibrated method and 2f/1f technique are displayed in Fig. 9b. To make the comparison clearer, three segments of data arrowed by b-1, b-2 and b-3 are enlarged. In this experiment, the measured concentration drifts from 499.2 ppm to 507.6 ppm (1.68%) without calibration in a period of 1.5 hours. Such drift is improved to 0.02% (from 499.2 ppm to 499.3 ppm) by the 2f/1f technique and 0.14% (from 499.5 ppm to 500.2 ppm) by the self-calibrated method. Obviously, the

self-calibrated method and 2f/1f technique can effectively suppress the drift effects, and if we only focus on the data, it seems that the performance of 2f/1f technique is better than the self-calibrated method proposed in this study. However, considering the measuring accuracy informed by the 1σ standard deviation, the effectiveness of these two methods should be comparable to our experience. Honestly, the self-calibrated method really has an obvious limitation compared with the 2f/1f technique. Because the pulse signal and absorption-induced second harmonic signal are collected at different moments within the same scanning cycle, this method is more effective in eliminating influence from low-frequency drift. However, the calibration would fail in cases when high-frequency interference occurs within the same scanning cycle, for example the sudden disturbance as enlarged in Fig. 9 b-3. In the moment of high-frequency fluctuation, the self-calibrated results as labeled by arrows show a sharp vibration. However, the results from 2f/1f technique are relatively stable. To address such high-frequency optical fluctuation and circuit jitter, increasing the scanning frequency (sawtooth frequency) of WMS systems would be a good choice. Another limitation of the self-calibrated method comes from the broadening of absorption line shape in conditions of high pressure and high concentration, the pulse signal may also contain absorption information. As a result, the calibration effect will be weakened. As a countermeasure, we can increase the wavelength scanning range to move the pulse signal far away from the absorption region. Considering that more and more researchers choose sinusoidal signals to realize the wavelength scanning in DAS or WMS systems, it should be noted that the self-calibrated method would fail if the laser scanning is realized by a sine wave instead of the sawtooth signal, because the impulse function of $\delta(t)$ in Eq. (4) would disappear. So, if you intend to apply the new method to improve the detection stability, then the sawtooth wave is essential to drive the laser diode. In addition to the above limitations, the new method proposed in this study also has advantage over the 2f/1f technique that it only needs one channel of lock-in amplifier. Considering that the 2f/1f technique from Hanson group has been verified robust as a “gold standard” by many studies and widely used to engineering applications. The self-calibrated method has potential as well for wide applications to eliminate influence from optical fluctuation and circuit drift.

V. CONCLUSION

Long-term stability and drift are indeed a challenging issue in gas sensor development, as they can affect the accuracy and reliability of the sensor's measurement over extended periods of time. Researchers and engineers in this field work towards developing innovative solutions to mitigate and minimize the impact of drift on gas sensor performance. Although temperature control of the optical path and circuitry can greatly reduce sensor's measurement drift, the temperature control unit will significantly increase the system's power consumption which is limited in specific applications of intrinsic safety. In this study, we proposed a new self-calibrated method to WMS-based gas sensing system. Compared with the previous method, the major advantage is that the calibration signal and absorption signal are perfectly synchronized, enabling the complete

suppression of all interference from the optical path to electronic circuit. Compared with the robust 2f/1f technique, only one lock-in amplifier channel is required in our method which makes the sensor configuration very straightforward. The feasibility and effectiveness of the new method have been experimentally validated, achieving an excellent calibration result. Moreover, this method is not limited to methane detection alone, it is applicable to all gas detection based on WMS technology.

DECLARATION OF COMPETING INTEREST

The authors declare no conflicts of interest on this study.

REFERENCES

- [1] Q. J. Wang, P. S. Sun, Z. R. Zhang, Y. J. Cai, W. B. Huang, T. Pang, B. Wu, H. Xia, Q. Guo, “Method of adaptive wide dynamic range gas concentration detection based on optimized direct absorption spectroscopy,” *Opt. Express*, 2023, 31(10): 16770-16780.
- [2] Y. F. Ma, T. T. Liang, S. D. Qiao, X. N. Liu, and Z. T. Lang, “Highly sensitive and fast hydrogen detection based on light-Induced thermoelastic spectroscopy,” *Ultrafast Sci*, 2023, 3, 0024.
- [3] J. M. Dang, J. H. Zhang, X. J. Dong, L. J. Kong, and H. Y. Yu, “A trace CH₄ detection system based on DAS calibrated WMS technique,” *Spectrochim. Acta, Part A*, 2022, 266, 120418.
- [4] N. W. Liu, L. G. Xu, S. Zhou, L. Zhang, and J. S. Li, “Simultaneous detection of multiple atmospheric components using an NIR and MIR laser hybrid gas sensing system,” *ACS Sens.* 2020, 5(11), 3607–3616.
- [5] F. Wang, J. Wu, Y. Cheng, L. Fu, J. Zhang, and Q. Wang, “Simultaneous detection of greenhouse gases CH₄ and CO₂ based on a dual differential photoacoustic spectroscopy system,” *Opt. Express*, 2023, 31, 33898-33913.
- [6] M. Yang, Z. Wang, Q. X. Nie, K. Ni, and W. Ren, “Mid-infrared cavity-enhanced absorption sensor for ppb-level N₂O detection using an injection-current-modulated quantum cascade laser,” *Opt. Express*, 2021, 29(25), 41634–41642.
- [7] M. Raza, L. Ma, C. Y. Yao, M. Yang, Z. Wang, Q. Wang, R. F. Kan, W. Ren, “MHz-rate scanned-wavelength direct absorption spectroscopy using a distributed feedback diode laser at 2.3 μm ,” *Opt Laser Technol*, 2020, 130: 106344.
- [8] R. Liang, F. P. Wang, Q. S. Xue, Q. Wang, J. H. Wu, Y. P. Cheng, Q. Li, “A Fourier-domain-based line shape recovery method used in direct absorption spectroscopy,” *Spectrochim. Acta A Mol. Biomol. Spectrosc*, 2022, 275: 121153.
- [9] J. M. Supple, E. A. Whittaker, W. Lenth, “Theoretical description of frequency modulation and wavelength modulation spectroscopy,” *Appl. Opt.* 1994, 33(27): 6294-6302.
- [10] S. Schilt, L. Thévenaz, P. Robert, “Wavelength modulation spectroscopy: combined frequency and intensity laser modulation,” *Appl. Opt.* 2003, 42(33): 6728-6738.
- [11] F. P. Wang, R. Liang, Q. S. Xue, Q. Wang, J. H. Wu, Y. P. Cheng, J. C. Sun, Q. Li. “A novel wavelength modulation spectroscopy gas sensing technique with an ultra-compressed wavelength scanning bandwidth,” *Spectrochim. Acta A Mol. Biomol.* 2022, 280: 121561.
- [12] U. Platt J. Stutz. “Differential absorption spectroscopy. Springer Berlin Heidelberg,” 2008.
- [13] Y. Wang, Y. Wei, T. Liu, T. Sun, K. T. Grattan, “TDLAS Detection of Propane/Butane Gas Mixture by Using Reference Gas Absorption Cells and Partial Least Square Approach,” *IEEE Sens*, 2018, 18(20): 8587-8596.
- [14] A. Farooq, et al., “Laser sensors for energy systems and process industries: Perspectives and directions,” *Progress in Energy and Combustion Science*, 2022, 91: 100997.
- [15] C. Liu, et al., “Laser absorption spectroscopy for combustion diagnosis in reactive flows: A review,” *Applied Spectroscopy Reviews*, 2019, 54 (1): 1-44.
- [16] C. S. Goldenstein, et al., “Infrared laser-absorption sensing for combustion gases,” *Progress in Energy and Combustion Science*, 2017, 60: 132-176.
- [17] Z. Wang, et al., “Application of 2D temperature measurement to a coal-fired furnace using CT-TDLAS,” *Measurement Science and Technology*, 2019, 31 (3): 035203.
- [18] W. Y. Peng, et al., “Single-ended mid-infrared laser-absorption sensor for time-resolved measurements of water concentration and temperature within

- the annulus of a rotating detonation engine,” *Proceedings of the Combustion Institute*, 2019, 37 (2): 1435-1443.
- [19] A. Upadhyay, et al., “Tomographic imaging of carbon dioxide in the exhaust plume of large commercial aero-engines,” *Applied Optics*, 2022, 61 (28): 8540-8552.
- [20] F. P. Wang, J. Chang, C. G. Zhu, Z. L. Wang, Y. N. Liu, W. Wei, Y. B. Wei, H. Jiang, “Demodulation algorithm used in single-beam system immune to light power drift,” *Appl. Opt.*, 2015, 54(8): 2032-2038.
- [21] G. J. Tu, Y. Wang, F. Z. Dong, H. Xia, T. Pang, Z. R. Zhang, B. Wu, “Novel method for correcting light intensity fluctuation in the TDLAS system,” *Chin Opt Lett*, 2012, 10(4): 042801.
- [22] G. B. Rieker, J. B. Jeffries, R. K. Hanson, “Calibration-free wavelength-modulation spectroscopy for measurements of gas temperature and concentration in harsh environments,” *Appl. Opt.*, 2009, 48(29): 5546-5560.
- [23] C. S. Goldenstein, et al., “Fitting of calibration-free scanned-wavelength-modulation spectroscopy spectra for determination of gas properties and absorption lineshapes,” *Applied Optics*, 2014, 53 (3): 356-367.
- [24] G. Enemali, et al., “Cost-Effective Quasi-Parallel Sensing Instrumentation for Industrial Chemical Species Tomography,” *IEEE Transactions on Industrial Electronics*, 2022, 69 (2): 2107-2116.
- [25] K. Owen, A. Farooq, “A calibration-free ammonia breath sensor using a quantum cascade laser with WMS 2f/1f,” *Appl. Phys. B*, 2014, 116: 371-383.
- [26] N. W. Liu, L. G. Xu, J. S. Li, “Self-calibrated wavelength modulation spectroscopy based on 2 f/1 f amplitude and integral area for trace gas sensing,” *Opt Quant Electron*, 2023, 55(1): 22.
- [27] T. Tomberg, M. Vainio, T. Hieta, L. Halonen, “Sub-parts-per-trillion level sensitivity in trace gas detection by cantilever-enhanced photo-acoustic spectroscopy,” *Scientific reports*, 2018, 8(1): 1848.
- [28] Z. Wang, Q. Wang, H. Zhang, S. Borri, L. Galli, A. Sampaolo, P. Patimisco, V. L. Spagnolo, P. De Natale, W. Ren, “Doubly resonant sub-ppt photoacoustic gas detection with eight decades dynamic range,” *Photoacoustics*, 2022, 27: 100387.
- [29] J. C. Sun, J. Chang, Q. D. Zhang, F. P. Wang, Z. F. Zhang, Y. M. Fan, L. B. Tian, “Recovery integral absorption method in the full concentration range to eliminate the interference of background gas,” *Spectrochim. Acta A Mol. Biomol*, 2022, 267: 120553.

Fupeng Wang received the Ph.D. degree in optical engineering from Shandong University, Jinan, China, and the University of Washington, Seattle, WA, USA, in 2019.

He is currently an Assistant Professor at the Ocean University of China, Qingdao, China. His research interests include tunable laser absorption spectroscopy (TDLAS), photoacoustic spectroscopy (PAS), nondispersive infrared spectroscopy (NDIR), and spectroscopy-based engineering applications in ocean detection and atmosphere analysis.

Jinghua Wu was born in Dezhou, Shandong, China, in 1999. He received the bachelor's degree in optoelectronic information science and engineering from the Nanyang Institute of Technology, Nanyang, China, in 2021.

He is engaged in the nondispersive infrared CO₂ sensor development and application for ocean detection.

Qiang Wang received the B.S. degree in electronic science and technology and Ph.D. degree in optical engineering from Shandong University, Jinan, China, in 2011 and 2016, respectively.

After his graduate study, he worked as a Postdoctoral Fellow at the Chinese University of Hong Kong, Hong Kong, and the Max Planck Institute of Quantum Optics, Munich, Germany. He is currently a Full Professor with the State Key Laboratory of Applied Optics of Changchun Institute of Optics, Fine Mechanics and Physics, Chinese Academy of Sciences, Changchun, China. His recent research interests include laser spectroscopy, optical sensing, and engineering application of trace gas analysis in atmosphere, deep sea, and public health.

Qian Li was born in Weihai, China, in 1993. He received the B.S. degree in electrical engineering and automation engineering from the Harbin Institute of Technology (HIT), Harbin, China, in 2015, and the Ph.D. degree in circuits and systems from the Changchun Institute of Optics, Fine Mechanics and Physics, Chinese Academy of Sciences, Changchun, China, in 2010.

He is currently a Lecturer with the College of Information Science and

Engineering, Ocean University of China, Qingdao, China. He is mainly engaged in weak signal detection.

Diansheng Cao received the Ph.D. degree in mechanical manufacturing and automation engineering from Changchun Institute of Optics, Fine Mechanics and Physics, (CIOMP), Chinese Academy of Sciences (CAS), Changchun, China, in 2012.

He is currently an Associate Professor at the Ocean University of China, Qingdao, China. His research interests include high-spectral-resolution instrument design, optical measurement instruments, optical remote sensing instruments, and optical remote sensing data processing.

Qingsheng Xue received the Ph.D. degree in optical engineering from the Changchun Institute of Optics, Fine Mechanics and Physics, Chinese Academy of Sciences, Changchun, China, in 2010.

He is currently a Professor at the Ocean University of China, Qingdao, China. His research interests include optical design, hyperspectral imaging, and development and applications of optical instruments for ocean detection.